Analytical Biochemistry 414 (2011) 47–57

Contents lists available at ScienceDirect

Analytical Biochemistry

journal homepage: www.elsevier.com/locate/yabio

Characterization of side reactions during the annealing of small interfering RNAs

Stephan Seiffert, Harald Debelak, Philipp Hadwiger, Kerstin Jahn-Hofmann, Ingo Roehl, Hans-Peter Vornlocher, Bernhard Noll *

Roche Kulmbach, GmbH, D-95326 Kulmbach, Germany

ARTICLE INFO

Article history:
Received 9 November 2010
Received in revised form 25 February 2011
Accepted 25 February 2011
Available online 2 March 2011

Keywords:
siRNA
Oligonucleotide
Ion-pair reversed-phase HPLC
Size-exclusion chromatography
Duplex stability
Mass spectrometry

ABSTRACT

Small interfering RNAs (siRNAs) are emerging as a novel therapeutic modality for the specific inhibition of target gene expression. The development of siRNA-based therapeutics requires in-depth knowledge of the manufacturing process as well as adequate analytical methods to characterize this class of molecules. Here the impurity formation during the annealing of siRNA was investigated. Two siRNAs containing common chemical RNA modifications (2′-*O*-methyl, 2′-deoxy-2′-fluoro, 2′-deoxy-ribose, and phosphorothioate linkages) were used to determine major side reactions—such as 2′,3′-isomerization, strand scission, and HF elimination—depending on annealing parameters such as RNA concentration, presence of cations, temperature, and time. Individual impurities were characterized using analytical size exclusion chromatography, denaturing and nondenaturing ion-pair reversed-phase high-performance liquid chromatography, differential scanning calorimetry, and ultraviolet spectrometry. The degradation pathways described in this work can lead to significantly reduced product quality and compromised drug activity. The data reported here provide background to successfully address challenges associated with the manufacture of siRNAs and other nucleic acid therapeutics such as aptamers, spiegelmers, and decoy and antisense oligonucleotides.

RNA interference (RNAi)[1] is a natural process to regulate gene expression. RNAi has been discovered in worms [1], but it became obvious that previously described posttranscriptional gene silencing in plants [2] and fungi [3] involves the same cellular mechanism. To date, RNAi has been described for nearly all eukaryotic species, including humans [4]. In a stepwise order of cellular events involving sequence-dependent target recognition and enzymatic cleavage, RNAi leads to the down-modulation of a specific messenger RNA (mRNA). The natural RNAi mechanism can be triggered by so-called small interfering RNA (siRNA), short helical RNA molecules that are generated in the cell from larger double-stranded RNA precursors by enzymatic nucleolysis [5]. RNAi can also be triggered very effectively by introducing chemically synthesized siRNA into living cells, circumventing several upstream RNA processing steps of the natural pathway [4]. RNAi has quickly become an important tool in molecular biology to analyze protein function and to identify novel therapeutic targets. Various siRNA molecules are currently under clinical investigation as promising therapeutic agents to treat diseases, including cancer, viral infection, and ocular disease [6–10].

siRNA molecules are formed by two at least partially complementary single strands, namely the passenger strand and the guide strand, with typical strand lengths of 19–23 nucleotides and usually contain 19–21 base pairs and two nucleotide 3′ overhangs at both ends. Into siRNA molecules intended for therapeutic use, several chemical modifications are typically introduced to abrogate immunomodulatory potential, increase nuclease stability, and/or improve systemic circulation half-life [11–13]. Most common chemical modifications include 2′-*O*-methyl, 2′-deoxy-2′-fluoro, and 2′-deoxy modifications at the ribose and phosphorothioate linkages [14,15]. Chemical modifications are crucial for the development not only of siRNA therapeutics but also of other nucleic acid drugs such as aptamers and decoy and antisense oligonucleotides [16]. Each nucleic acid single strand can be chemically synthesized stepwise from the 3′ terminus to the 5′ terminus employing conventional solid-phase phosphoramidite chemistry. After completion of synthesis, the strands are cleaved from the solid support and deprotected, yielding the crude RNA single strands that are usually purified by anion exchange high-performance liquid chromatography (AEX–HPLC) and desalted [17,18]. The final

* Corresponding author. Fax: +49 0 9221 827 62 8999.
E-mail addresses: bernhard.noll@roche.com, bernhard_noll@gmx.de (B. Noll).

[1] *Abbreviations used:* RNAi, RNA interference; mRNA, messenger RNA; siRNA, small interfering RNA; AEX–HPLC, anion exchange high-performance liquid chromatography; CNET, N3-cyanoethyl-thymidine-nucleoside; N+But, RNA strand containing incompletely deprotected guanine bases; PAGE, polyacrylamide gel electrophoresis; CGE, capillary gel electrophoresis; IP–RP, ion-pair reversed-phase; MS, mass spectrometry; PBS, phosphate-buffered saline; PS-1, passenger strand of siRNA-1; PS-2, passenger strand of siRNA-2; GS-1, guide strand of siRNA-1 and siRNA-2; RT, room temperature; SEC, size exclusion chromatography; UV, ultraviolet; ACN, acetonitrile; HFIP, 1,1,1,3,3,3,-hexafluoro-2-propanol; TEA, triethylamine; ESI, electrospray ionization; T_m, melting temperature; DSC, differential scanning calorimetry; M_r(parent), molecular weight of the parent molecule; RRT, relative retention time.

0003-2697/$ - see front matter © 2011 Elsevier Inc. All rights reserved.
doi:10.1016/j.ab.2011.02.040

siRNA duplex is then formed by mixing the two purified single strands in near equimolar ratio in aqueous solution, typically followed by a heating and cooling phase (i.e., annealing).

Expected impurities resulting from the linear synthesis of the single strands are (i) shortmer sequences (N−*x*; e.g., N−1, N−2) [19–21], (ii) longmer sequences (N+*x*; e.g., N+G, N+A) [22], (iii) incompletely deprotected sequences or strands containing modified bases resulting from the synthesis process (N+; e.g., CNET, N+But) [23,24], and (iv) sequences in which a sulfur atom at a phosphorothioate linkage is exchanged by an oxygen atom (PO) [25]. In addition to the impurities generated during synthesis, deprotection, and purification of the single strands, more side products are formed during the annealing process, largely promoted by elevated temperatures and buffer components. Possible side reactions include phosphoryl migration from the 3′-carbon to the 2′-carbon of the ribose moiety, strand scission at phosphodiester bonds adjacent to 2′-OH groups [26], and elimination of HF in 2′-deoxy-2′-fluoro-modified RNA [27–29]. All guide and passenger strand impurities present in the annealing mixture will contribute to the complexity of the impurity profile of the resulting duplex. In a mixture of two complementary siRNA strands, duplex formation occurs quickly. The resulting siRNA solution typically contains optimal duplex (i.e., full-length passenger strand hybridized with full-length guide strand) and nonoptimal duplex (i.e., duplex containing guide and/or passenger strand impurities). Nonhybridized strands comprise the single-strand fraction. The annealing process is intended to minimize the presence of nonoptimal duplex in the mixture. Heating of the solution to temperatures where a substantial fraction of the duplexes is completely dissociated followed by a period of slow cooling favors the formation of the thermodynamically preferred optimal duplexes, whereas single-strand impurities may remain nonhybridized. In theory, an optimal annealing process would result in the maximal amount of optimal double strand in the duplex fraction.

The annealing step, together with the purity of the individual single strands after synthesis and purification, defines the overall quality of the siRNA duplex. However, annealing conditions of nucleic acids have not been studied as extensively as the conditions of chemical synthesis of single strands. This may be due in part to the lack of high-resolution analytical methods that do not denature the siRNA duplex during analysis. Although a number of methods have been reported for the physicochemical characterization of single-stranded oligonucleotides under denaturing conditions such as polyacrylamide gel electrophoresis (PAGE), capillary gel electrophoresis (CGE) [30,31], AEX–HPLC [32–35], and ion-pair reversed phase (IP–RP) HPLC that can be coupled to mass spectrometry (MS) detection [21,24,36,37], only a few methods that enable characterization of the hybridized duplex under nondenaturing conditions (i.e., without disrupting the existing double strand) have been described. To our knowledge, CGE [38] and IP–RP HPLC coupled with MS detection [39–41] have been reported to allow high-resolution separations under nondenaturing conditions.

In this work, we have used a variety of denaturing and nondenaturing methods to study side reactions during the annealing process and to characterize the annealed duplex of two siRNAs containing the most common chemical modifications. The aim of our study was to establish procedures to control the annealing process and/or minimize impurity formation and obtain the largest amounts of the thermodynamically preferred optimal duplex. We investigated the major side reactions responsible for impurity formation of siRNA and studied the main factors affecting the formation of the duplex (i.e., strand concentration, salt concentration, and annealing temperature). The formation of the RNA degradation products described in this work can result in reduced drug quality and may significantly compromise the activity of not only siRNA but also other nucleic acid therapeutics such as aptamers, spiegelmers, and decoy as well as antisense oligonucleotides.

Materials and methods

Chemicals

Acetonitrile (chromatography grade) was purchased from Biosolve (Valkenswaard, The Netherlands). Methanol (chromatography grade), 1,1,1,3,3,3-hexafluoro-2-propanol (puriss. p.a.), sodium bromide (puriss. p.a.), sodium phosphate (ultrapure), and triethylamine (puriss. p.a.) were purchased from Fluka (Sigma–Aldrich, St. Louis, MO, USA). 10× Phosphate-buffered saline (PBS, pH 7.4) was purchased from Gibco/Life Technologies (Carlsbad, CA, USA). $MgCl_2$ solution (1 M) was obtained from Ambion/Life Technologies (Carlsbad, CA, USA). NaCl solution (5 M, ultrapure) was purchased from Sigma–Aldrich. A Milli-Q 185 Plus apparatus (Millipore, Bedford, MA, USA) was used to prepare deionized water (>18 MΩ cm) for all solutions and mobile phases.

RNA

The three single-stranded oligonucleotides PS-1, PS-2, and GS-1 were synthesized by conventional solid-phase synthesis. The sequence of passenger strand PS-1 is 5′-cuuAcGcuGAGuAcuucGATT-3′, the sequence of passenger strand PS-2 is 5′-*cuu*A*c*G*cu*GA-G*u*A*cuuc*GATT-3′, and the sequence of guide strand GS-1 is UCGAAGuACUcAGCGuAAGTT, where uppercase letters indicate 2′-OH RNA nucleotides, lowercase letters indicate 2′-*O*-methyl nucleotides, lowercase italic letter indicate 2′-deoxy-2′-fluoro-nucleotides, and underlined letters indicate 2′-deoxy nucleotides connected via a phosphorothioate linkage. siRNA-1 is a double-stranded RNA formed by the two single strands GS-1 and PS-1. siRNA-2 is a double-stranded RNA formed by the two single strands GS-1 and PS-2 (Fig. 1). The guide strand sequence is complementary to the mRNA of firefly luciferase. The major impurity markers N−1, N−2, and N+G, as well as a complete set of 2′,5′-isomers for GS-1 and PS-1, were synthesized. Sequences are listed in Tables 2 and S2. All oligoribonucleotides were manufactured at Roche Kulmbach GmbH (Kulmbach, Germany).

Annealing and thermal incubation

Solutions of siRNA or RNA single strands (100 μM) were incubated for the indicated time in the respective medium in closed single tubes or 96-well plates in a Thermomixer or Mastercycler (Eppendorf, Hamburg, Germany). Incubation temperatures are

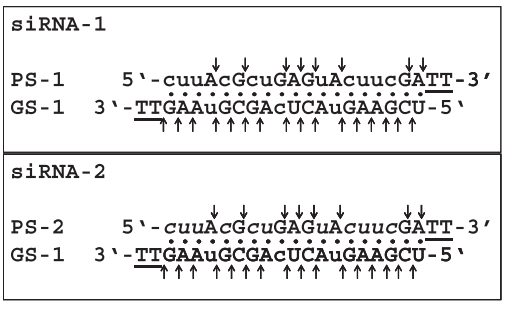

Fig.1. siRNA-1 (upper panel) and siRNA-2 (lower panel). Uppercase letters indicate 2′-OH RNA nucleotides, lowercase letters indicate 2′-*O*-methyl nucleotides, lowercase italic letters indicate 2′-deoxy-2′-fluoro-nucleotides, underlined letters indicate 2′-deoxy nucleotides connected via a phosphorothioate linkage, dots indicate Watson–Crick base pairing, and arrows indicate scission sites in 4-h incubations of siRNA or the respective single strands at 85 °C in 100-μM solutions containing 1 mM $MgCl_2$.

indicated in Results. Annealing steps included heating for 10 min and cooling to room temperature (RT) over a period of 3 h. For degradation studies, incubation was stopped instantly after the indicated time by dilution with cold water. Until analysis, all solutions were stored at +2 to +8 °C.

Size exclusion chromatography

Size exclusion chromatography (SEC) was carried out on a Dionex Ultimate 3000 RS series HPLC system (Dionex, Sunnyvale, CA, USA) using ultraviolet (UV) detection at 260-nm. Oligoribonucleotides were separated on a Superdex 75 column (10/300 GL, GE Healthcare, Pollars Wood, UK) at RT. Mobile phase consisted of 1× PBS containing 10% acetonitrile (ACN). The flow rate was 0.75 ml/min. The injection volume was 5 µl of a 50-µM RNA solution in 1× PBS.

Ion-pair reversed-phase HPLC

For IP–RP HPLC separations, samples of single- and double-stranded nucleic acids were applied to an Ultimate 3000 RS series HPLC system (Dionex, Sunnyvale, CA, USA) using UV detection at 260-nm. Oligoribonucleotides were separated by methanol gradient elution on an XBridge C18 OST column (2.1 × 50 mm, 2.5 µm particle size, Waters, Milford, MA, USA). Mobile Phase A consisted of 100 mM 1,1,1,3,3,3,-hexafluoro-2-propanol (HFIP), 16.3 mM triethylamine (TEA), and 1% methanol. Mobile phase B consisted of 100 mM HFIP, 16.3 mM TEA, and 95% methanol. For nondenaturing applications, the column temperature was 20 °C. The gradient was run from 6 to 35% of mobile phase B in 15 min at a flow rate of 250 µl/min. The injection volume was 2 µl of a 50-µM RNA solution in 1× PBS. For denaturing applications, the column temperature was 65 °C for single-stranded RNA and 75 °C for double-stranded RNA. A gradient was run from 1 to 18% of mobile phase B in 30 min at a flow rate of 250 µl/min. The injection volume was 20 µl of a 5-µM RNA solution in water.

Anion exchange chromatography

For AEX–HPLC separations, samples were applied to an Ultimate 3000 RS series HPLC system (Dionex) using UV detection at 260-nm. Oligoribonucleotides were separated by salt gradient elution on a DNAPac-200 4 × 250-mm column (Dionex). Mobile phase A consisted of 20 mM sodium phosphate buffer (pH 11.0) and 10% ACN. Mobile phase B consisted of 20 mM sodium phosphate buffer (pH 11.0), 1.0 M NaBr, and 10% ACN. The gradient was run from 35 to 50% of mobile phase B in 15 min at a flow rate of 1 ml/min. The injection volume was 10 µl of a 10-µM RNA solution in 1× PBS.

Mass spectrometry

For MS analysis, an LCQ Deca XP+ Ion Trap mass spectrometer equipped with an electrospray ionization (ESI) interface (Thermo Fisher Scientific, Waltham, MA, USA) was used in line with the IP–RP HPLC system. The mass spectrometer was run in negative ion mode, the spray voltage was 4.5 V, the capillary temperature was 315 °C, the capillary voltage was −100 V, and the scanning mass range was 600–2000 *m*/*z*. Data acquisition and analysis was performed using Xcalibur software and ProMass Deconvolution software (Thermo Fisher Scientific).

Differential scanning calorimetry

Melting temperature (T_m) values of concentrated RNA solutions were determined using a NanoDSC instrument (Waters). Solutions were prepared in water or 150 mM NaCl, adjusted to the indicated concentrations, degassed, and filled into the capillary. Heating/cooling cycles between 20 and 95 °C were applied with a scan rate of 1 °C/min. DSCRun software (version 4.0.5) was used for data acquisition. NanoAnalyze (version 2.1.6) was used for data analysis.

UV-spectroscopy

T_m values of diluted RNA solutions were determined using a DU 800 spectrophotometer (Beckman Coulter, Brea, CA, USA) at 260-nm. The temperature range of the measurements was 20–95 °C with a ramp rate of 0.5 °C/min. Data acquisition and analysis was performed using the instrument software (version 2.0).

Results

Impact of temperature on composition of single- and double-stranded fractions of siRNA-1 and siRNA-2

Annealing of siRNA was performed using a small excess of single strand (typically 1–7% of total RNA), leading to the formation of siRNA duplex and an additional fraction of nonhybridized single strand. The effect of the annealing temperature on the composition of these fractions was studied using 100-µM solutions of siRNA-1 and siRNA-2 (Fig. 1) in 1× PBS or water. Solutions were heated to 60, 75, 85, and 95 °C for 10 min, allowed to cool to RT over a period of 3 h, and subsequently analyzed by SEC–UV and nondenaturing IP–RP HPLC. Controls were incubated at room temperature. Percentages of total single strand and duplex were recorded by SEC–UV (Fig. 2), and percentages of full-length nonhybridized passenger strand and duplex were recorded by IP–RP HPLC (Fig. 3) (see Table 1). For both siRNAs, the percentages of duplex relative to total RNA as measured by nondenaturing IP–RP HPLC were slightly higher than those from SEC. Correspondingly, the single-strand fraction was approximately 2% lower in IP–RP HPLC than in SEC. This difference may be a consequence of the improved separation efficiency of IP–RP HPLC. Individual nonhybridized single-strand impurities might not reach the detection threshold of the IP–RP method, and as a consequence the percentage of total single strand may appear to be lower than the percentage measured by SEC. For both siRNAs, duplex content did not change with incubation temperature. However, full-length nonhybridized passenger strand decreased significantly (up to 1% relative to total RNA) with increasing annealing temperature. At the same time, a corresponding increase in earlier eluting impurities was detected in the single-strand fraction for both siRNAs. Using MS detection, the impurities were identified as the 5′N−1 PS-1 shortmer and strands with the same molecular weight as PS-1, most likely isomers of this strand (Fig. 3). Similar results were obtained using an excess of guide strand (data not shown). To estimate the stability of nonoptimal duplexes, several process-related impurities were synthesized (5′N−1, 5′N−2, N+G, and 2′,5′-isomers of PS-1 and GS-1) and T_m values of duplexes containing these strands were determined by differential scanning calorimetry (DSC) at RNA concentrations of 100 µM (Table 2). In water, the 5′N−1 PS-1 containing nonoptimal duplex showed a decrease in T_m of 4.2 °C compared with the optimal duplex. The largest decrease in T_m was seen in duplexes containing 2′,5′-isomers. Depending on the position of the 2′,5′-linkage, the decrease in T_m was as high as 10.3 °C, which is in agreement with data from the literature [42]. Importantly, the differences in T_m between nonoptimal duplexes and optimal duplex appeared to be larger in salt-free solution than in 150 mM NaCl (Table 2).

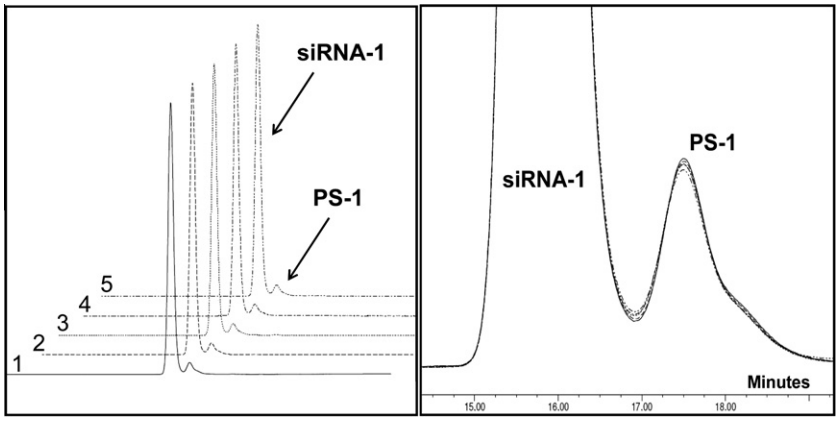

Fig.2. Impact of annealing temperature on siRNA-1 composition. SEC of samples after annealing at RT (trace 1), 60 °C (trace 2), 70 °C (trace 3), 85 °C (trace 4), and 95 °C (trace 5) is shown. All annealing steps were performed using 100-μM siRNA in 1× PBS. The main single-strand peak (PS-1) and double-strand peak (siRNA-1) are indicated by arrows. No change in the PS-1 single-strand peak was observed with annealing temperature (the right panel displays zoomed and overlaid traces).

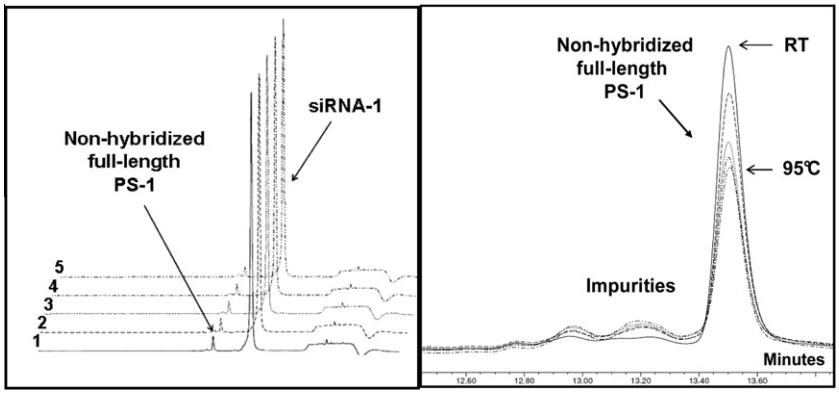

Fig.3. Impact of annealing temperature on siRNA-1 composition. IP–RP HPLC of samples after annealing at RT (trace 1), 60 °C (trace 2), 70 °C (trace 3), 85 °C (trace 4), and 95 °C (trace 5) is shown. All annealing steps were performed using 100-μM siRNA in 1× PBS. The main single-strand peak (PS-1) and double-strand peak (siRNA-1) are indicated by arrows. The full-length PS-1 peak was most pronounced in the RT incubations and decreased with increasing incubation temperatures (the right panel displays zoomed and overlaid traces). The impurity peaks contained 5′N–1 PS-1 (M_r(parent)-320) and 2′,5′ PS-1 isomers (M_r(parent)) and increased with incubation temperatures. They were most pronounced in the 95 °C incubations.

Table 1
Impact of annealing temperature on composition of siRNA-1 (upper panel) and siRNA-2 (lower panel).

Annealing temperature (%)	Duplex (peak area %)		Total single strand (peak area %)	PS-1 FLP (peak area %)
	SEC	IP–RP	SEC	IP–RP
SiRNA-1				
RT	94.2	96.5	5.8	2.6
60 °C	94.3	96.5	5.7	2.4
70 °C	94.3	96.7	5.7	2.1
85 °C	94.3	96.7	5.7	1.9
95 °C	94.4	96.7	5.6	1.8
siRNA-2				PS-2 FLP (peak area %)
RT	94.2	95.4	6.6	3.6
60 °C	94.3	95.4	6.6	3.5
70 °C	94.3	95.5	6.7	3.3
85 °C	94.3	95.5	6.7	3.1
95 °C	94.4	95.5	6.7	2.6

Note. Annealing steps were performed at RT and 60, 70, 85, and 95 °C using 100-μM siRNA in 1× PBS with a slight excess of passenger strand. Duplex content of the samples was determined by SEC and nondenaturing IP–RP HPLC. Total single strand was determined by SEC, and nonhybridized full-length passenger strand (PS-1 FLP or PS-2 FLP) was determined by nondenaturing IP–RP HPLC.

Concentration-dependent changes in duplex T_m

The influence of RNA concentration and presence of cations on duplex stability of siRNA-1 and siRNA-2 was investigated. siRNA solutions were prepared at concentrations of 4, 20, 100, and 500 μM in water and 150 mM sodium chloride. T_m was used as the measure for duplex stability and determined using UV-spectroscopy or DSC. In all solutions of siRNA-1 and siRNA-2 in 150 mM NaCl, T_m was above 80 °C. The difference in T_m between the highest concentration (500 μM) and lowest concentration (4 μM) was approximately 6 °C for both siRNAs (Table 3). In water, duplex stability was significantly lower than in saline and strongly dependent on RNA concentration. T_m at the lowest concentration was approximately 32 °C for siRNA-1 and 40 °C for siRNA-2. The difference in T_m values between the highest and lowest concentrations was approximately 35 °C for both siRNAs (Table 3). In water, 100-μM solutions (the concentration used in most incubations) of siRNA-1 and siRNA-2 were dissociated at temperatures of 60 °C and above, whereas in 150 mM NaCl, the duplex form was prevalent at 60 and 70 °C. At 85 °C, approximately half of the duplexes were dissociated in saline (Table 3). Solutions containing 1 mM $MgCl_2$ showed T_m values similar to those of saline (data not shown).

Table 2
Differences in T_m values between optimal duplex siRNA-1 and nonoptimal duplex variants of siRNA-1 containing major impurity markers.

Duplex ID	Description	5′-Sequence-3′ of non-optimal strand	ΔT_m in water (°C)	ΔT_m in PBS (°C)
	PS-1	cuuAcGcuGAGuAcuucGATT		
Variant P-short1	5′N−1 PS-1 shortmer	uuAcGcuGAGuAcuucGATT	4.2	1.4
Variant P-short2	5′N−2 PS-1 shortmer	uAcGcuGAGuAcuucGATT	4.3	1.6
Variant P-iso1	PS-1-Isomer 1	cuu**A**cGcuGAGuAcuucGATT	7.2	3.0*
Variant P-iso2	PS-1-Isomer 5	cuuAcGcuGA**G**uAcuucGATT	10.3	3.0*
Variant P-long1	N+G11 PS-1 longmer	cuuAcGcuGAGGuAcuucGATT	2.8	nd
	GS-1	UCGAAGuACUcAGCGuAAGTT		
Variant G-short1	5′N-1 GS-1 shortmer	CGAAGuACUcAGCGuAAGTT	0.8	0.3
Variant G-short2	5′N-2 GS-1 shortmer	GAAGuACUcAGCGuAAGTT	2.8	1.2
Variant G-iso1	GS-1-Isomer 2	U**C**GAAGuACUcAGCGuAAGTT	3.4	0.0*
Variant G-iso2	GS-1-Isomer 9	UCGAAGuAC**U**cAGCGuAAGTT	8.9	3.0*
Variant G-long1	N+G6 GS-1 longmer	UCGAAGGuACUcAGCGuAAGTT	3.0	nd
Variant G-long2	N+G13 GS-1 longmer	UCGAAGuACUcAGGCGuAAGTT	4.5	nd

Note. Measurements were performed by DSC using 50-μM solutions in water or 1× PBS. Uppercase letters indicate 2′-OH RNA nucleotides, lowercase letters indicate 2′-*O*-methyl nucleotides, underlined letters indicate 2′-deoxy-nucleotides connected via a phosphorothioate linkage, bold uppercase letters indicate 2′-5′-connected nucleotides, nd indicates that measurements were not done, and * indicates measurements by UV-spectroscopy using 4-μM solutions in 1× PBS.

Table 3
T_m values (°C) of siRNA-1 and siRNA-2.

Solution	siRNA-1		siRNA-2	
	Water	NaCl	Water	NaCl
4 μM	31.8	80.6	40.1	84.1
20 μM	43.1	82.5	50.7	85.5
100 μM	52.2	84.2	59.3	87.7
500 μM	67.1	86.9	75.3	90.6

Note. T_m values of 4-μM siRNA in water or 150 mM NaCl were measured using thermal UV-spectroscopy. T_m values of all other solutions were determined using DSC.

Thermal degradation of 2′-O-methyl-modified duplex siRNA-1

The influence of incubation time and temperature on the formation of single-strand impurities was investigated in 100-μM solutions of siRNA-1, GS-1, or PS-1 in water, 150 mM NaCl, or 1 mM $MgCl_2$. Solutions were heated to 60, 70, and 85 °C for 1, 2, or 4 h and subsequently analyzed by denaturing IP–RP HPLC and AEX–HPLC. Controls were incubated at RT. In the controls, no significant impurity formation was detected over the whole 4-h period (Fig. 4, upper and middle panels, trace 1). At elevated temperatures, the resulting chromatograms showed a distinct impurity peak in front of the guide strand (GS-1) as well as the passenger strand (PS-1) (peaks I and i in Fig. 4, upper and middle panels, traces 2–4). In water, these novel peaks were detected after incubation of single strands as well as after duplex incubations. Peak area increased with incubation time and temperature. The percentage values obtained by IP–RP HPLC and AEX–HPLC were very similar (0.6 and 0.1% at 60 °C, 1.5 and 1.6% at 70 °C, and 8.0 and 8.9% at 85 °C, respectively). The molecular weights of the generated impurities were identical to those of the respective parent peaks (M_r was 6751.3 for peak I and 6777.4 for peak i), suggesting an isomerization process as the source of these side products. To further investigate the characteristics of possible impurities, all isomers of GS-1 and PS-1 containing a single 2′,5′-linkage were chemically synthesized. Retention time and relative retention time (RRT) were determined by denaturing IP–RP HPLC and denaturing AEX–HPLC. In the IP–RP HPLC, most 2′,5′-isomers eluted earlier than the main peak but were not separated to baseline levels. However, full resolution of main peaks (GS-1 and PS-1) and impurity peaks was achieved using a denaturing AEX–HPLC (see Table S2). Employing this method, synthetic single 2′,5′-isomers of PS-1 and GS-1 could be separated to baseline from the respective parent peaks. In IP–RP analysis, the measured RRT values of the synthetic 2′,5′-isomers for PS-1 were between 0.989 and 0.994, and those for GS-1 were between 0.986 and 1.003. In AEX chromatography, RRT values were between 0.941 and 0.974 for the PS-1 isomers and between 0.928 and 0.988 for the GS-1 isomers. These values closely matched the RRTs of the impurity peaks in IP–RP analysis (0.993 for PS-1 and GS-1) and AEX analysis (0.946–0.975 for PS-1 and 0.959–0.979 for GS-1) (see Table S2). These data further substantiate phosphoryl migration (2′,5′-isomer formation) as the major source of impurities in this experiment.

In water, no significant difference in the extent of impurity formation was detected between incubations of single- and double-strand samples. Impurity formation increased linearly with time (Fig. 5). After single-strand incubations of GS-1 and PS-1, impurity levels were very similar in water and saline. In solutions containing 1 mM $MgCl_2$, a large percentage of shorter RNA fragments was detected, suggesting scission of the RNA backbone during incubation (Fig. 6). For both strands, cleavage reactions at all 3′ positions of the unmodified 2′-OH nucleotides were detected by MS (Fig. 1 and Table S2). In saline, only small amounts of strand scission were detected, predominantly in GS-1, which has 16 unmodified RNA nucleotides compared with 8 unmodified RNA nucleotides in PS-1. No significant degree of strand scission was detected after incubation in water. In the duplex experiments, a considerable difference between water incubations and incubations containing salt was detected. In 150 mM NaCl or 1 mM $MgCl_2$, significant amounts of side products were found only after incubations at 85 °C (Fig. 7). The T_m values of the respective solutions indicate that isomerization, as well as strand scission, was inhibited by stable duplex formation (Table 3). Although the detected side products were the same as in the respective single-strand incubations (Fig. 6), the amounts in the duplex incubations were lower (Fig. 7).

Thermal degradation of 2′-O-methyl and 2′-deoxy-2′-fluoro-modified duplex siRNA-2

The influence of incubation time and temperature on the formation of single-strand impurities was investigated in 100-μM solutions of siRNA-2, GS-1, or PS-2 in water, 150 mM NaCl, or 1 mM $MgCl_2$. Solutions were heated to 60, 70, and 85 °C for 1, 2, or 4 h and subsequently analyzed by denaturing IP–RP HPLC. Controls were incubated at room temperature. In the controls, no significant impurity formation was detected over a 4-h period. At elevated temperatures, the peak profile of the guide strand (GS-1) in the

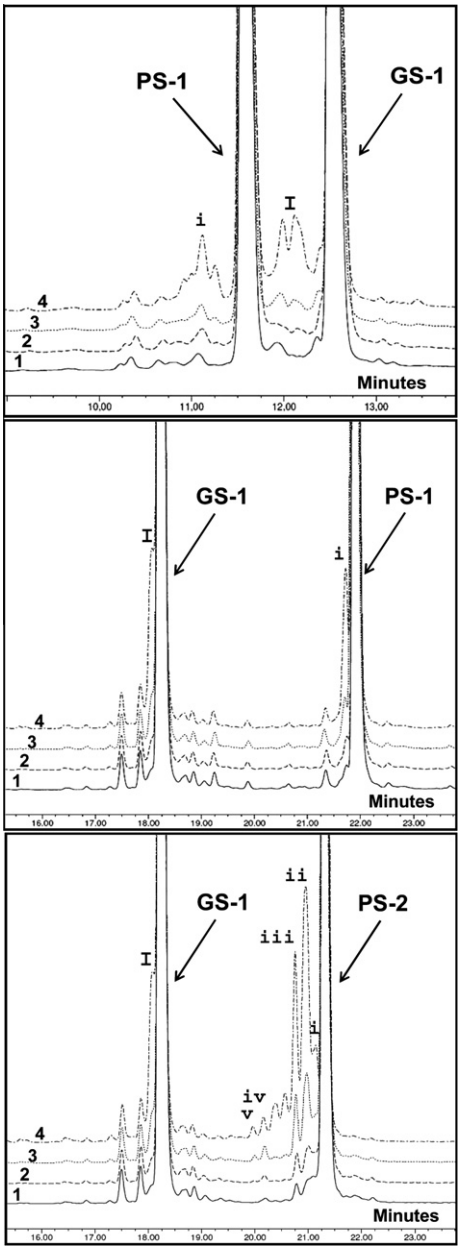

Fig.4. Denaturing AEX–HPLC of siRNA-1 (upper panel), denaturing IP–RP–HPLC of siRNA-1 (middle panel), and siRNA-2 (lower panel) after incubations at RT (trace 1), 60 °C (trace 2), 70 °C (trace 3), and 85 °C (trace 4). All incubations were carried out for 4 h using 100-μM siRNA solutions in water. The full-length guide strand peak (GS-1) and passenger strand peak (PS-1 or PS-2) are indicated by arrows. Impurity peaks are marked by uppercase letters (guide strand) and lowercase letters (passenger strands). I indicates 2′,5′-isomers of GS-1, i indicates 2′,5′-isomers of PS-1 or PS-2, ii and iii indicate HF elimination products of PS-2 (M_r(parent)-2 and M_r(parent)-4), and iv and v indicate HF elimination products of PS-2 (M_r(parent)-20).

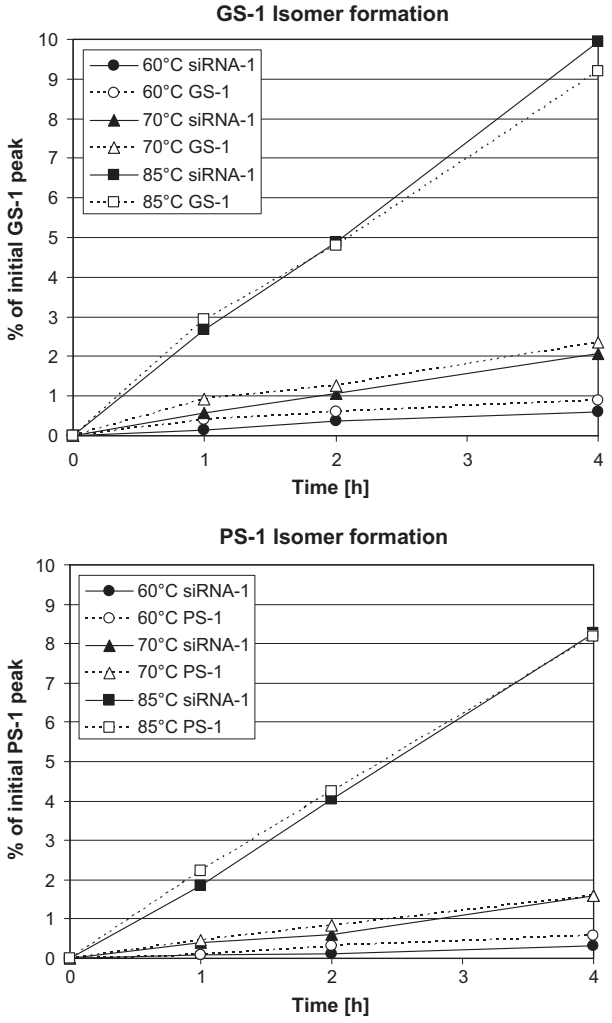

Fig.5. Isomer levels of guide (upper panel) and passenger strand (lower panel) after single-strand (GS-1 or PS-1) or double-strand (siRNA-1) incubations in water. All incubations were performed using 100-μM siRNA solutions.

chromatograms of siRNA-2 was nearly identical to the peak profile of GS-1 in the chromatograms of siRNA-1 that were recorded earlier (Fig. 4). As in the siRNA-1 incubations, the impurity peak in front of the guide strand (I) showed the same molecular weight as the parent peak (M_r was 6751.3). The extent of GS-1 isomer formation in the siRNA-2 incubations was similar to that in the siRNA-1 incubations (Fig. 7, upper panel, and Fig. 8, upper panel). Compared with PS-1, the extent of isomer formation was lower for passenger strand PS-2 (Fig. 4, peak i; Fig. 7 and Fig. 8, middle panels). However, PS-2 displayed several additional impurity peaks (ii, iii, iv, and v in Fig. 4, lower panel). The two major impurity peaks eluted at RRTs of 0.985 and 0.975 (peaks ii and iii in Fig. 4, lower panel). These impurities showed a molecular weight loss of 2 and 4 compared with PS-2. The two impurity peaks at RRTs of 0.950 and 0.940 displayed a loss of 20 compared with PS-2 (peaks iv and v in Fig. 4, lower panel). M_r values recorded between RRTs of 0.952 and 0.975 included multiples and combinations of weight losses of 2 and 20. Similar to the incubations of siRNA-1 and its single strands, the presence of Mg^{2+} ions in solutions of siRNA-2 and PS-2 resulted in considerable amounts of strand scission in addition to the other side reactions. All possible products of phosphodiester cleavage reactions at the 3′ ends of the unmodified 2′-OH nucleotides of PS-2 were detected by MS analysis (Fig. 1; see also Table S3 in supplementary material). Impurity formation of the 2′-deoxy-2′-fluoro-modified strand was inhibited by the same conditions as was isomerization (Fig. 8), suggesting an impact of the duplex structure on the underlying mechanism.

Discussion

Impact of temperature on composition of single- and double-strand fractions of siRNA-1 and siRNA-2

In practice, duplex content of synthetic siRNA is rarely 100%. Usually a small single-digit percentage of the strands remains non-

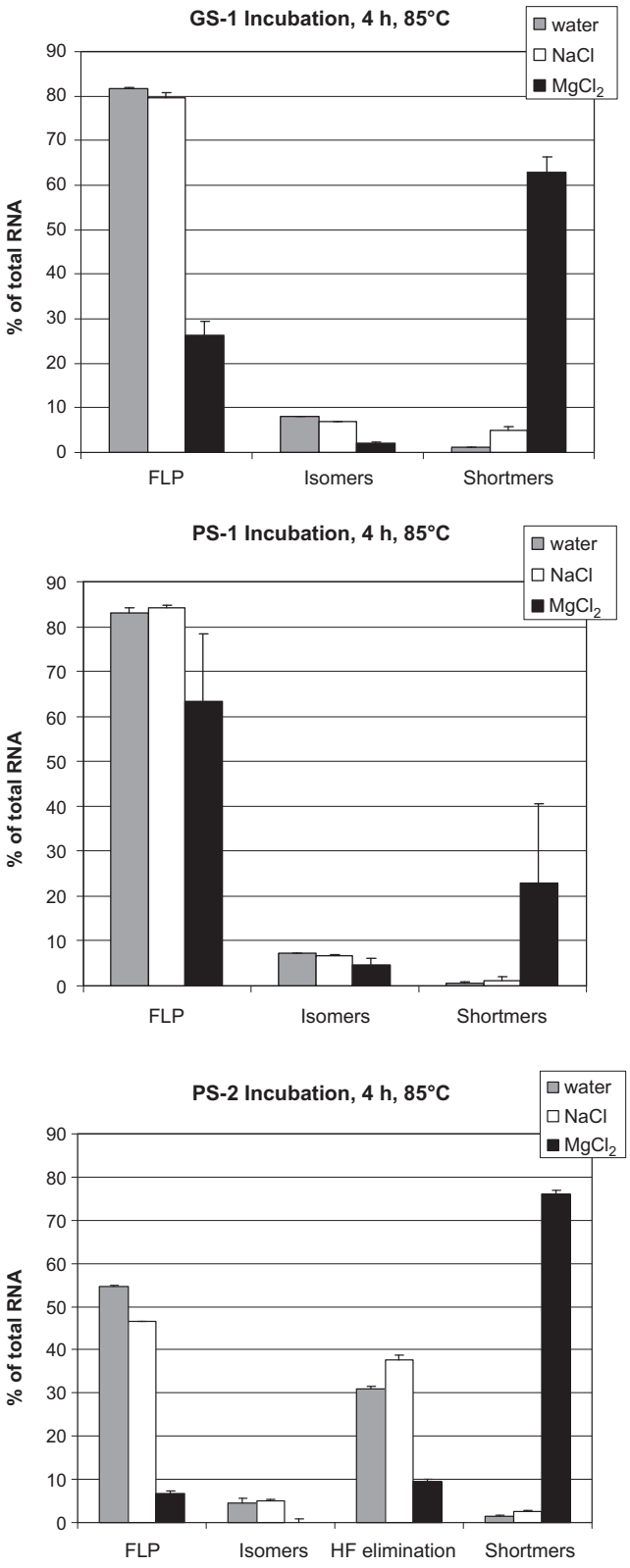

Fig.6. Side products of single strands GS-1 (upper panel), PS-1 (middle panel), and PS-2 (lower panel) as quantified by denaturing IP–RP–HPLC after incubation at 85 °C. All incubations were carried out for 4 h using 100-μM siRNA solutions in water, 150 mM NaCl, and 1 mM $MgCl_2$. Mean values from two independent experiments are shown.

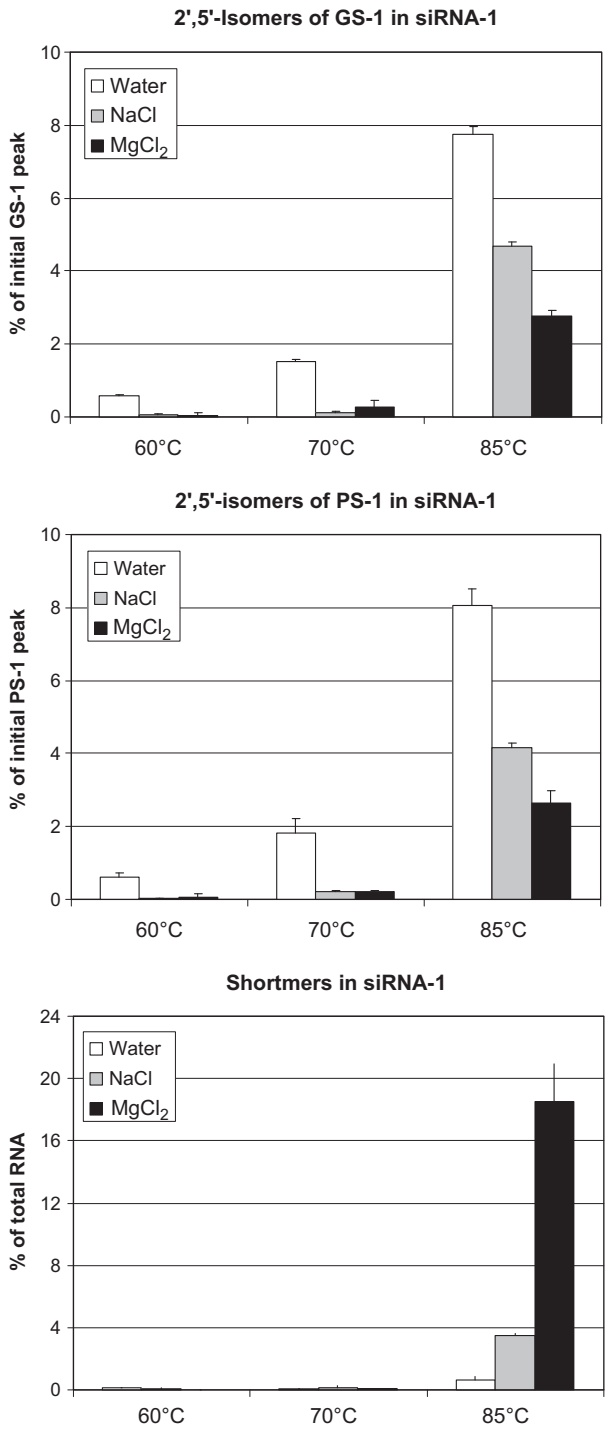

Fig.7. Side products of siRNA-1 as quantified by denaturing IP–RP–HPLC after incubation at 60, 70, and 85 °C. All incubations were carried out for 4 h using 100-μM siRNA solutions in water, 150 mM NaCl, and 1 mM $MgCl_2$. Mean values from two independent experiments are shown.

hybridized after the annealing procedure. In annealing experiments using siRNA-1 and siRNA-2, duplex content of both siRNAs appeared to be independent of temperature (Table 1). However, although no effect on the percentages of total duplex was observed, a significant change in the nonhybridized full-length single-strand fraction was detected for both siRNAs using nondenaturing IP–RP HPLC. As annealing temperature increased, the percentage of nonhybridized full-length single strand decreased. At the same time, the percentage of nonhybridized isomers and shortmers increased. The largest changes were measured at the highest temperature, suggesting that annealing

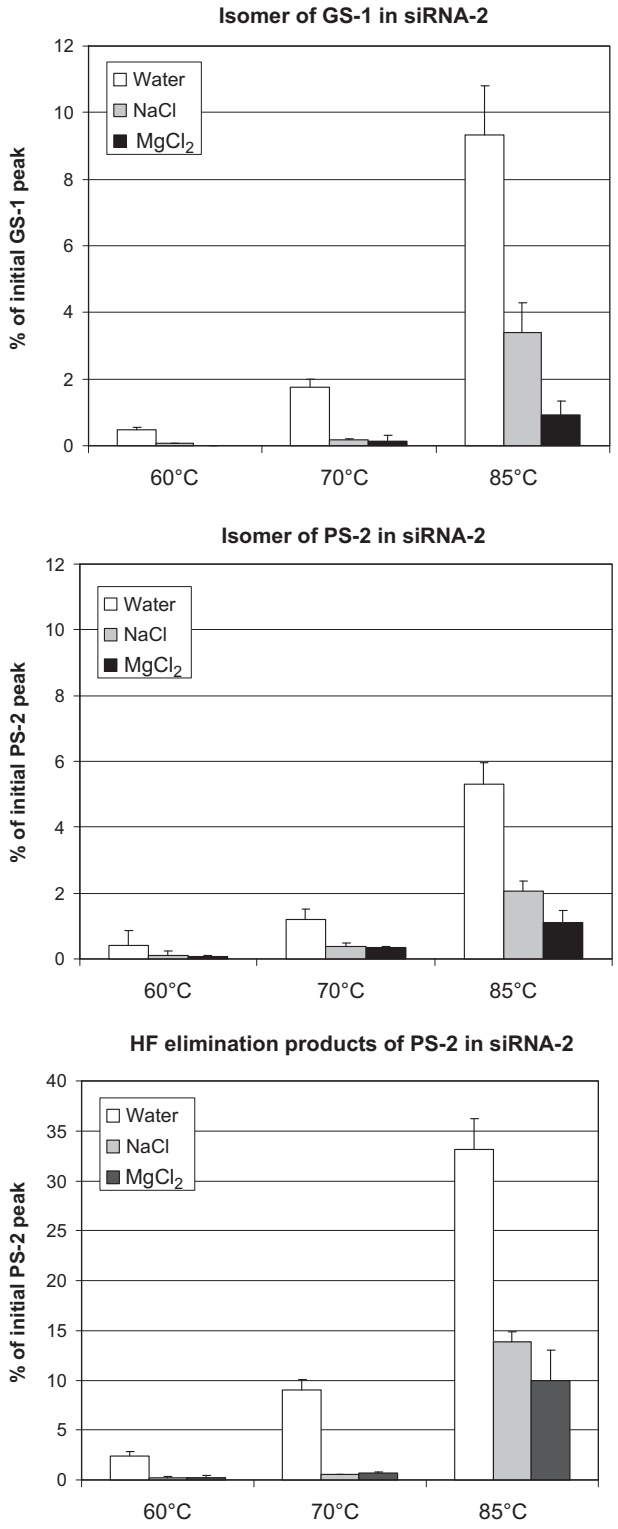

Fig.8. Side products of siRNA-2 as quantified by denaturing IP–RP HPLC after incubation at 60, 70, and 85 °C. All incubations were carried out for 4 h using 100-μM solutions in water, 150 mM NaCl, and 1 mM $MgCl_2$. Mean values from two independent experiments are shown.

at temperatures close to or above the T_m of the duplex enables redistribution of nonhybridized full-length single strand to the duplex fraction. As a consequence, the amount of optimal duplex in the siRNA mixture increased as annealing temperature increased without significant changes in the overall amount of duplex. When optimal duplex was compared with nonoptimal duplexes (i.e., duplexes containing shortmers, longmers, or isomers), T_m differences were larger in water than in 150 mM NaCl (Table 3). A difference in T_m between optimal and nonoptimal duplexes favors redistribution of single strand between the duplex and single-strand fraction. These results indicate that annealing in water facilitates the formation of optimal duplex in the mixture.

Concentration-dependent changes of duplex T_m

In water, T_m values of siRNA-1 and siRNA-2 were significantly lower than those in saline (Table 3). In addition, a strong dependency of the T_m on strand concentration was observed in the salt-free solutions. This finding was attributed to the second-order kinetics of the annealing reaction that favors the duplex form at higher concentrations [43]. The effect is stronger in solutions where the duplex is not further stabilized by the presence of salt. This has two important implications for the annealing step of siRNA. First, it demonstrates that stable duplex formation can be achieved at ambient temperature in solutions of siRNA that do not contain salt provided that the respective siRNA concentration is sufficiently high. As a consequence, for a given siRNA in salt-free solution, the T_m can be set by simply adjusting the RNA concentration. Second, it indicates that in salt-free solutions at concentrations typically used for UV-spectroscopic measurements, the duplex can be partially dissociated. Due to the different extinction coefficients of double strands and single strands, unaccounted dissociation can result in significant variations in the UV readout when temperatures are close to the T_m of the duplex solution. This must be taken into account when determining siRNA concentration in water.

Thermal degradation of 2′-O-methyl-modified duplex siRNA-1

Incubation of single-stranded guide strand (GS-1) or passenger strand (PS-1) at elevated temperatures resulted in the formation of one major impurity peak for each strand in IP–RP analysis. The molecular weights of these impurities were identical to those of the respective parent compounds, suggesting an isomerization reaction as the source of these impurities (Fig. 4). To further investigate this finding, all possible isomers of PS-1 and GS-1 containing a single 2′,5′-linkage were chemically synthesized and analyzed using two different chromatographic methods: IP–RP HPLC and AEX–HPLC. Both techniques showed matching RRTs of the impurities and those of the synthetic 2′,5′-isomers (see Table S1). These results strongly support 2′,3′-phosphoryl migration as the major side reaction during annealing of siRNA-1. Percentages of the impurities were very similar for both chromatographic techniques, although the values may be slightly understated due to possible coelution with the parent peaks (Fig. 4). The mechanism of isomerization has been described previously and is in agreement with the conditions applied in our experiments. During isomerization, a penta-coordinated cyclic phosphate is formed on the nucleophilic attack of the 2′-hydroxy group of the ribose (pathway a in Fig. 9). Subsequent cleavage of the 3′-O–P bond yields the 2′,5′-isomer (pathway b in Fig. 9). Both reactions are reversible, and the 2′,5′-isomer as well as the 3′,5′-isomer can be generated from the penta-coordinated transition state [44,45]. To exclude base-catalyzed side reactions, which would be expected at basic pH [27,29], all incubations were performed in aqueous solutions at slightly acidic pH. In water and saline, 2′,5′-isomer formation was the main side reaction. In solutions containing Mg^{2+} ions, RNA shortmers were the dominant impurity species (Figs. 6 and 7). The shorter RNA fragments result from scission of the phosphate backbone. Strand scission occurred at all 2′-OH-unmodified nucleotides (Fig. 1 and Table S3) as Mg^{2+} ions appeared to function as

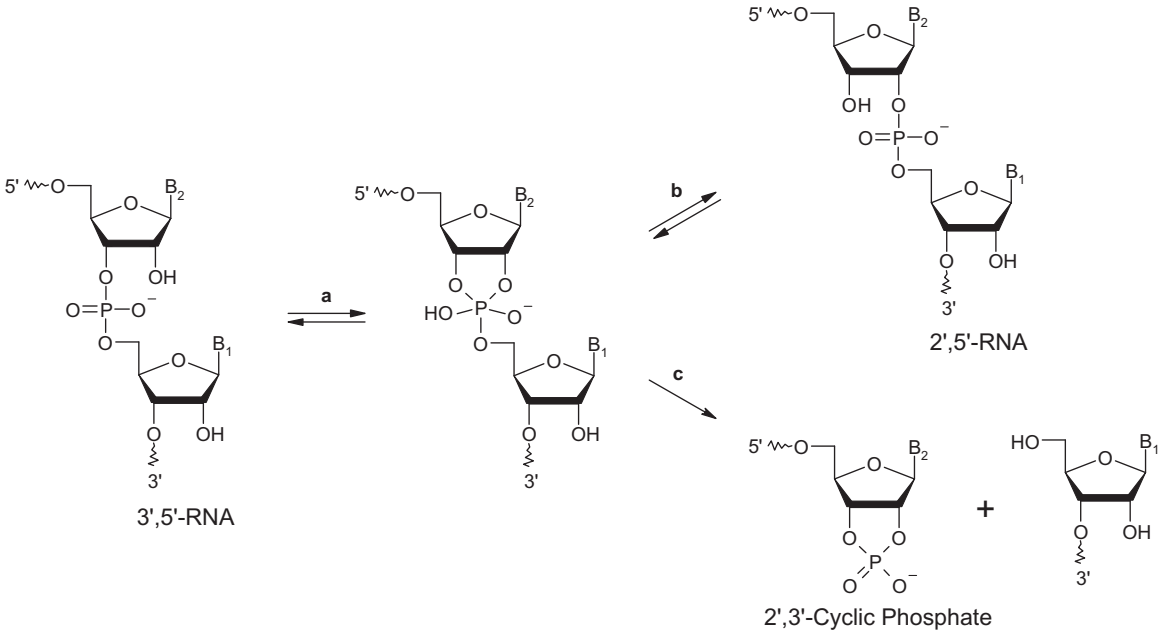

Fig.9. Putative reaction mechanism of 2′,3′-isomerization and strand scission involving a pentavalent transition state at the phosphate group. In the absence of divalent cations, reversible isomerization is preferred (reactions a and b). Divalent cations such as Mg^{2+} catalyze irreversible strand scission (pathway c).

metal catalysts for the cleavage of the phosphodiester bond. Metal ion-promoted hydrolysis of the phosphodiester bonds involves cleavage of the exocyclic P–O bond, resulting in the formation of a 2′,3′-cyclic phosphate and release of the 5′-linked nucleoside (reaction c in Fig. 9). Subsequent hydrolysis of the cyclic phosphate yields a mixture of 2′- and 3′-phosphates [45,46]. The exact locations of the isomerizations were not determined in our work. However, because strand scission occurred at all 2′-OH-unmodified nucleotides and formation of the 2′,5′-isomers is part of the same mechanism (involving a penta-coordinated cyclic transition state), isomerization is expected at all 2′-OH-unmodified nucleotides of the RNA strand. Our results indicate that both reactions, isomerization and strand scission, are temperature and time dependent and effectively inhibited by duplex formation. This is in agreement with the published mechanisms of isomerization and strand scission [26].

Thermal degradation of 2′-O-methyl- and 2′-deoxy-2′-fluoro-modified duplex siRNA-2

The type and extent of impurity formation detected for guide strand GS-1 in incubations of siRNA-2 were essentially the same as in incubations of siRNA-1, suggesting that side reactions for a given RNA strand are similar in siRNAs containing a different complementary strand (Figs. 7 and 8). However, total impurity formation of the 2′-deoxy-2′-fluoro-modified passenger strand (PS-2) was found to be significantly different from impurity formation of its 2′-*O*-methyl-modified counterpart (PS-1). Several additional impurity peaks eluting in front of the 2′,5′-isomer peak were detected in duplex as well as in single-strand incubations of PS-2 (Fig. 4). In water and saline, these impurities were the major degradation products of PS-2 (Figs. 6 and 8). The detected molecular weights suggested an elimination reaction at the

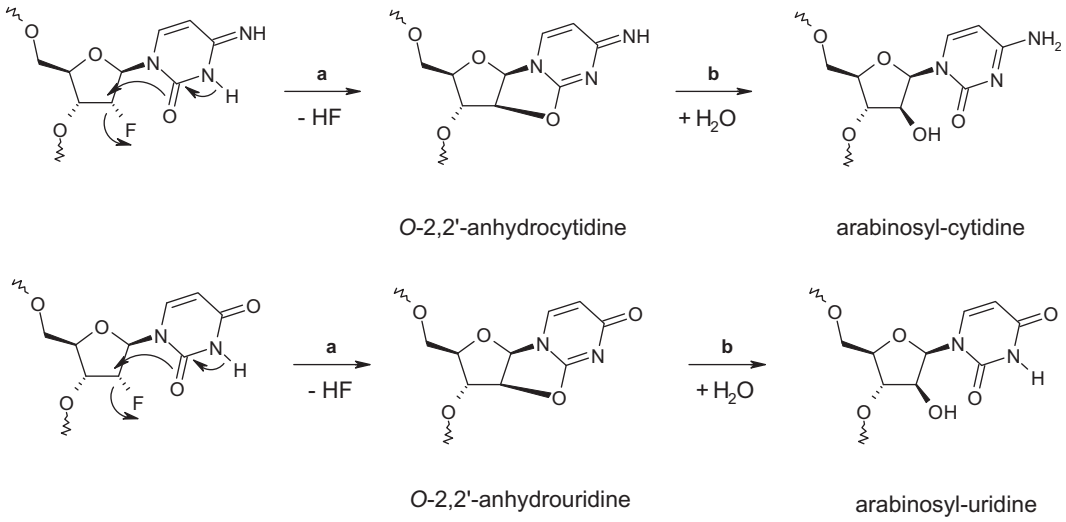

Fig.10. Putative reaction mechanisms of HF elimination from 2′-deoxy-2′-fluoro-cytidine (upper scheme) and 2′-deoxy-2′-fluoro-uridine (lower scheme). HF elimination (pathway a) results in the cyclic intermediate *O*-2,2′-anhydro-nucleotide (M_r(parent)-20). Subsequent hydrolysis (pathway b) yields the arabinosyl-nucleotide (M_r(parent)-2).

2′-fluoro-modified pyrimidines as the source of the impurities. HF elimination proceeds via a cyclic transition state (*O*-2,2′-anhydronucleotide, M_r(parent)-20), subsequently generating the 2′-OH hydrolysis product (arabinosyl-nucleotide, M_r(parent)-2) [27–29] (Fig. 10). In addition to impurities resulting from a single elimination reaction, combinations of one or more elimination reactions per RNA molecule were detected (e.g., M_r(parent)-4, M_r(parent)-22, M_r(parent)-24, M_r(parent)-40). HF elimination occurred in parallel with isomerization and strand scission. PS-2 contains five 2′-deoxy-2′-fluoro-cytidines and six 2′-deoxy-2′-fluoro-uridines. The exact locations of the eliminations in the strands were not determined. Similar to the formation of the 2′,5′-isomers, HF elimination was promoted by elevated temperatures, increased with time, and was effectively inhibited by duplex formation (Fig. 8). Similar to incubations of siRNA-1, strand scission in siRNA-2 occurred at all 2′-OH-unmodified nucleotides (Fig. 1 and Table S3).

Conclusions

The reported results have significant implications with regard to annealing conditions for siRNAs and other RNAs with defined secondary structure in molecular biology, diagnostic, and (most important) therapeutic applications. The degradation pathways described in this work can lead to significantly reduced product quality and compromised drug activity. In addition, our findings apply not only to siRNA but also to other nucleic acid therapeutics, including aptamers, spiegelmers, and decoy and antisense oligonucleotides.

Based on our data, incubation temperature and time, as well as the presence of divalent cations, are the most critical factors in controlling impurity formation. Without metal ion catalysts, formation of 2′,5′-isomers was the major side reaction of the two RNA single strands containing 2′-unmodified nucleotides (GS-1 and PS-1). The impact of isomerization on the quality of the duplex was aggravated when heating and cooling cycles were repeated. In our experiments, 10 successive heating and cooling cycles from 20 to 95 °C resulted in a 10 °C decrease in T_m of the annealing mixture, which corresponds to the difference in T_m of optimal duplex and nonoptimal duplex containing 2′,5′-isomers. For the 2′-deoxy-2′-fluoro-modified strand (PS-2), HF elimination at the modified pyrimidine nucleotides was the dominant side reaction. When Mg^{2+} ions were present, metal ion-catalyzed degradation of all three investigated RNA strands was observed to a significant extent. All side reactions (isomerization, elimination, and strand scission) were suppressed by duplex formation.

Because impurity formation was most pronounced at elevated temperatures, heating of the siRNA solution should be limited to the lowest temperature required for substantial dissociation of the duplex. A slow cooling process after duplex dissociation promotes the formation of the thermodynamically preferred optimal duplex. The optimal annealing temperature, therefore, may be close to the T_m of the duplex. Divalent cations such as Mg^{2+} catalyze strand scission and are best avoided in the annealing solution. Performing annealing in salt-free solution allows effective annealing at lower temperatures compared with solutions containing salt. In addition, the differences in T_m of nonoptimal duplex compared with optimal duplexes appeared to be greater in salt-free solutions, facilitating the redistribution of imperfectly matched impurities to the single-strand fraction. The strong concentration dependency of the T_m in salt-free solutions allows adjustment of the T_m by changing the siRNA concentration. Therefore, it is recommended to determine the T_m of an individual siRNA duplex at different concentrations before setting the final annealing temperature. Taken together, annealing in salt-free solutions allows lower annealing temperatures, minimizes side reactions, and simplifies lyophilization of the resulting siRNA molecule.

Acknowledgment

The authors thank Mario Klobedanz and Frank Hertel for their excellent technical support and laboratory assistance.

Appendix A. Supplementary data

Supplementary data associated with this article can be found, in the online version, at doi:10.1016/j.ab.2011.02.040.

References

[1] A. Fire, S. Xu, M.K. Montgomery, S.A. Kostas, S.E. Driver, C.C. Mello, Potent and specific genetic interference by double-stranded RNA in *Caenorhabditis elegans*, Nature 391 (1998) 806–811.
[2] C. Napoli, C. Lemieux, R. Jorgensen, Introduction of a chimeric chalcone synthase gene into petunia results in reversible co-suppression of homologous genes in trans, Plant Cell 2 (1990) 279–289.
[3] C. Cogoni, G. Macino, Posttranscriptional gene silencing in *Neurospora* by a RecQ DNA helicase, Science 286 (1999) 2342–2344.
[4] S.M. Elbashir, J. Harborth, W. Lendeckel, A. Yalcin, K. Weber, T. Tuschl, Duplexes of 21-nucleotide RNAs mediate RNA interference in cultured mammalian cells, Nature 411 (2001) 494–498.
[5] G. Meister, T. Tuschl, Mechanisms of gene silencing by double-stranded RNA, Nature 431 (2004) 343–349.
[6] D. Bumcrot, M. Manoharan, V. Koteliansky, D.W. Sah, RNAi therapeutics: a potential new class of pharmaceutical drugs, Nat. Chem. Biol. 2 (2006) 711–719.
[7] A. de Fougerolles, H.P. Vornlocher, J. Maraganore, J. Lieberman, Interfering with disease: a progress report on siRNA-based therapeutics, Nat. Rev. Drug Discov. 6 (2007) 443–453.
[8] N. Durcan, C. Murphy, S.A. Cryan, Inhalable siRNA: potential as a therapeutic agent in the lungs, Mol. Pharmacol. 5 (2008) 559–566.
[9] T. Nguyen, E.M. Menocal, J. Harborth, J.H. Fruehauf, RNAi therapeutics: an update on delivery, Curr. Opin. Mol. Ther. 10 (2008) 158–167.
[10] M.E. Davis, J.E. Zuckerman, C.H. Choi, D. Seligson, A. Tolcher, C.A. Alabi, Y. Yen, J.D. Heidel, A. Ribas, Evidence of RNAi in humans from systemically administered siRNA via targeted nanoparticles, Nature 464 (2010) 1067–1070.
[11] M. Robbins, A. Judge, I. MacLachlan, siRNA and innate immunity, Oligonucleotides 19 (2009) 89–102.
[12] C.R. Allerson, N. Sioufi, R. Jarres, T.P. Prakash, N. Naik, A. Berdeja, L. Wanders, R.H. Griffey, E.E. Swayze, B. Bhat, Fully 2′-modified oligonucleotide duplexes with improved in vitro potency and stability compared to unmodified small interfering RNA, J. Med. Chem. 48 (2005) 901–904.
[13] M. Sioud, G. Furset, L. Cekaite, Suppression of immunostimulatory siRNA-driven innate immune activation by 2′-modified RNAs, Biochem. Biophys. Res. Commun. 361 (2007) 122–126.
[14] T.P. Prakash, B. Bhat, 2′-Modified oligonucleotides for antisense therapeutics, Curr. Top. Med. Chem. 7 (2007) 641–649.
[15] A. Judge, K. McClintock, J.R. Phelps, I. MacLachlan, Hypersensitivity and loss of disease site targeting caused by antibody responses to PEGylated liposomes, Mol. Ther. 13 (2006) 328–337.
[16] M. Faria, H. Ulrich, Sugar boost: when ribose modifications improve oligonucleotide performance, Curr. Opin. Mol. Ther. 10 (2008) 168–175.
[17] S.L. Beaucage, P.I. Radhakrishnan, Advances in the synthesis of oligonucleotides by the phosphoramidite approach, Tetrahedron 48 (1992) 2223–2311.
[18] B.S. Sproat, RNA synthesis using 2′-*O*-(*tert*-butyldimethylsilyl) protection, Methods Mol. Biol. 288 (2005) 17–32.
[19] J. Temsamani, M. Kubert, S. Agrawal, Sequence identity of the $n-1$ product of a synthetic oligonucleotide, Nucleic Acids Res. 23 (1995) 1841–1844.
[20] D. Chen, Z. Yan, D.L. Cole, G.S. Srivatsa, Analysis of internal ($n-1$)mer deletion sequences in synthetic oligodeoxyribonucleotides by hybridization to an immobilized probe array, Nucleic Acids Res. 27 (1999) 389–395.
[21] M. Gilar, Analysis and purification of synthetic oligonucleotides by reversed-phase high-performance liquid chromatography with photodiode array and mass spectrometry detection, Anal. Biochem. 298 (2001) 196–206.
[22] A.H. Krotz, P. Klopchin, K.L. Walker, S. Srivatsa, D.L. Cole, V.T. Ravikumar, On the formation of longmers in phosphorothioate oligodeoxyribonucleotide synthesis, Tetrahedron 38 (1997) 3875–3878.
[23] D.C. Capaldi, H. Gaus, A.H. Krotz, J. Arnold, R.L. Carty, M.N. Moore, A.N. Scozzari, K. Lowery, D.L. Cole, V.T. Ravikumar, Synthesis of high-quality antisense drugs: addition of acrylonitrile to phosphorothioate oligonucleotides: adduct characterization and avoidance, Org. Process Res. Dev. 7 (2003) 832–838.
[24] M. Gilar, K.J. Fountain, Y. Budman, J.L. Holyoke, H. Davoudi, J.C. Gebler, Characterization of therapeutic oligonucleotides using liquid chromatography with on-line mass spectrometry detection, Oligonucleotides 13 (2003) 229–243.

[25] A.H. Krotz, D. Gorman, P. Mataruse, C. Foster, J.D. Godbout, C.C. Coffin, A.N. Scozzari, Phosphorothioate oligonucleotides with low phosphate diester content: Greater than 99.9% sulfurization efficiency with "aged" solutions of phenylacetyl disulfide (PADS), Org. Process Res. Dev. 8 (2004) 852–858.
[26] S. Mikkola, U. Kaukinen, H. Lonnberg, The effect of secondary structure on cleavage of the phosphodiester bonds of RNA, Cell Biochem. Biophys. 34 (2001) 95–119.
[27] I.L. Doerr, J.J. Fox, Nucleosides. XXXIX: 2′-Deoxy-2′-fluorocytidine, 1-β-D-arabinofuranosyl-2-amino-1,4(2*H*)-4-iminopyrimidine, and related derivatives, J. Org. Chem. 32 (1967) 1462–1471.
[28] A. Krug, T.S. Oretskaya, E.M. Volkov, D. Cech, Z.A. Shabarova, A. Rosenthal, The behaviour of 2′-deoxy-2′-fluorouridine incorporated into oligonucleotides by the phosphoamidite approach, Nucleosides Nucleotides 8 (1989) 1473–1483.
[29] C.J. Calvitt, D.S. Levin, B.T. Shepperd, C.J. Gruenloh, Chemistry at the 2′ position of constituent nucleotides controls degradation pathways of highly modified oligonucleotide molecules, Oligonucleotides 20 (2010) 239–251.
[30] A.S. Cohen, A.J. Bourque, B.H. Wang, D.L. Smisek, A. Belenky, A nonradioisotope approach to study the in vivo metabolism of phosphorothioate oligonucleotides, Antisense Nucleic Acid Drug Dev. 7 (1997) 13–22.
[31] M. Gilar, A. Belenky, D.L. Smisek, A. Bourque, A.S. Cohen, Kinetics of phosphorothioate oligonucleotide metabolism in biological fluids, Nucleic Acids Res. 25 (1997) 3615–3620.
[32] A.J. Bourque, A.S. Cohen, Quantitative analysis of phosphorothioate oligonucleotides in biological fluids using direct injection fast anion-exchange chromatography and capillary gel electrophoresis, J. Chromatogr. B 662 (1994) 343–349.
[33] G.S. Srivatsa, P. Klopchin, M. Batt, M. Feldman, R.H. Carlson, D.L. Cole, Selectivity of anion exchange chromatography and capillary gel electrophoresis for the analysis of phosphorothioate oligonucleotides, J. Pharm. Biomed. Anal. 16 (1997) 619–630.
[34] W.J. Warren, G. Vella, Principles and methods for the analysis and purification of synthetic deoxyribonucleotides by high-performance liquid chromatography, Mol. Biotechnol. 4 (1995) 179–199.
[35] J.R. Thayer, V. Barreto, S. Rao, C. Pohl, Control of oligonucleotide retention on a pH-stabilized strong anion exchange column, Anal. Biochem. 338 (2005) 39–47.
[36] A. Apffel, J.A. Chakel, S. Fischer, K. Lichtenwalter, W.S. Hancock, Analysis of oligonucleotides by HPLC–electrospray ionization mass spectrometry, Anal. Chem. 69 (1997) 1320–1325.
[37] K.J. Fountain, M. Gilar, J.C. Gebler, Analysis of native and chemically modified oligonucleotides by tandem ion-pair reversed-phase high-performance liquid chromatography/electrospray ionization mass spectrometry, Rapid Commun. Mass Spectrom. 17 (2003) 646–653.
[38] L. Szekely, S. Kiessig, M.A. Schwarz, F. Kalman, Capillary gel electrophoresis of therapeutic oligonucleotides: analysis of single- and double-stranded forms, Electrophoresis 30 (2009) 1579–1586.
[39] M. Beverly, K. Hartsough, L. Machemer, Liquid chromatography/electrospray mass spectrometric analysis of metabolites from an inhibitory RNA duplex, Rapid Commun. Mass Spectrom. 19 (2005) 1675–1682.
[40] S.M. McCarthy, M. Gilar, J. Gebler, Reversed-phase ion-pair liquid chromatography analysis and purification of small interfering RNA, Anal. Biochem. 390 (2009) 181–188.
[41] J. Farand, F. Gosselin, De novo sequence determination of modified oligonucleotides, Anal. Chem. 81 (2009) 3723–3730.
[42] M. Wasner, D. Arion, G. Borkow, A. Noronha, A.H. Uddin, M.A. Parniak, M.J. Damha, Physicochemical and biochemical properties of 2′,5′-linked RNA and 2′,5′-RNA:3′,5′-RNA "hybrid" duplexes, Biochemistry 37 (1998) 7478–7486.
[43] V.A. Bloomfield, D.M. Crothers, I. Tinoco Jr., Nucleic Acids: Structures, Properties, and Functions, University Science Books, Sausalito, CA, 2000. pp. 259–334.
[44] H. Lonnberg, R. Stromberg, A. Williams, Compelling evidence for a stepwise mechanism of the alkaline cyclisation of uridine 3′-phosphate esters, Org. Biomol. Chem. 2 (2004) 2165–2167.
[45] S. Mikkola, E. Stenman, K. Nurmi, E. Yousefi-Salakdeh, R. Strömberg, H. Lönnberg, The mechanisms of the metal ion promoted cleavage of RNA phosphodiester bonds involves a general acid catalysis by the metal aquo ion on the departure of the leaving group, J. Chem. Soc. (1999) 1619–1625.
[46] I. Zagorowska, S. Kuusela, H. Lonnberg, Metal ion-dependent hydrolysis of RNA phosphodiester bonds within hairpin loops: a comparative kinetic study on chimeric ribo/2′- *O*-methylribo oligonucleotides, Nucleic Acids Res. 26 (1998) 3392–3396.